Local fatigue behavior in tapered areas of large offshore wind turbine blades

Raeis Hosseiny, Seyed Aydin; Jakobsen, Johnny

Published in:
37th Risø International Symposium on Materials Science

DOI (link to publication from Publisher):
10.1088/1757-899X/139/1/012022

Publication date:
2016

Document Version
Publisher's PDF, also known as Version of record

Local fatigue behavior in tapered areas of large offshore wind turbine blades

IOP Conf. Series: Materials Science and Engineering **139** (2016) 012022 doi:10.1088/1757-899X/139/1/012022

Local fatigue behavior in tapered areas of large offshore wind turbine blades

Seyed Aydin Raeis Hosseiny and Johnny Jakobsen

Department of Mechanical and Manufacturing Engineering, Aalborg University, Aalborg, Denmark

E-mail: aydin@m-tech.aau.dk

Abstract. Thickness transitions in load carrying elements lead to improved geometries and efficient material utilization. However, these transitions may introduce localized areas with high stress concentrations and may act as crack initiators that could potentially cause delamination and further catastrophic failure of an entire blade structure. The local strength degradation under an ultimate static loading, subsequent to several years of fatigue, is predicted for an offshore wind turbine blade. Fatigue failure indexes of different damage modes are calculated using a sub-modeling approach. Multi axial stresses are accounted for using a developed failure criterion with residual strengths instead of the virgin strengths. Damage initiation is predicted by including available Wöhler curve data of E-Glass fabrics and epoxy matrix into multi-axial fatigue failure criteria. As a result of this study, proper knock-down factors for ply-drop effects in wind turbine blades under multi-axial static and fatigue loadings can be obtained.

1. Introduction

Damage tolerant design of composites attracts attention of industry, owing to significantly reducing the maintenance costs in remote structures. Offshore wind turbine blades are designed to fulfil high endurance limits with minimum repair requirements+. Improving the effective life-time of the blades requires special considerations in areas, where continuous degradation of material characteristics due to high loading cycle is inevitable. Thickness transitions (ply-drops) are critical failure areas, because of local stress concentrations. Failure at ply-drops is largely dominated by interlaminar and transverse shear effects in the matrix [1, 2]. The process of failure can lead to ply delamination at relatively low applied strains under fatigue loading [3].

Among the current fatigue models in effect, fatigue life model and residual strength or stiffness models are formulated in macro-scale, while progressive damage model is defined in micro-scale [4, 5]. Progressive damage model is a computationally expensive method with inherent complexities. Additionally, obtaining the experimental data for generating sufficiently accurate Wöhler (S-N) curves and residual strength models is considerably time consuming [5]. A method of reducing computational and experimental cost in fatigue life prediction of multi-directional laminates through conducting experiments of different stress levels and geometries has been established [6]. By constructing a relationship between fatigue life and stress level for each stage, multi-axial damage index of a static strength failure criterion can predict the fatigue life of a general stacking sequence and ply orientation [5]. A relationship between damage evolution and remaining life of the composites, outlines the process of damage mechanism that would take place in the course of ultimate fracture [7]. Despite the promising applications of these

methods, they are mainly experimentally validated against constant amplitude tension fatigue type problems.

A vast amount of damage mechanisms in composite materials, force designers to consider the degraded stiffness and residual strength of blades, subjected to life-time fatigue in their calculations. This is typically done through design codes, where suitable knock-down factors are recommended. A new blade design has to fulfill its reliability under an extreme of a 20 years fatigue, followed by static loading to its ultimate limits. This particular loading scenario has been considered as an example for the present study. Local strength degradation and onset of damage in two selected ply-drop regions of the DTU 10 MW reference wind turbine [8] has been investigated. The blade geometry is provided in the form of an ABAQUS [9] finite element model with conventional layered shell elements (figure 1). Homogeneous anisotropic approximation of material properties are assigned to multidirectional laminates in the model, for simplicity [10, 11]. Composite layup is defined by partitioning the blade into 11 regions circumferentially (figure 2) and 100 regions radially [8]. The reference model considers the blade body as a prismatic beam passing through defined sections and does not consider the effect of tapering throughout the blade [8].

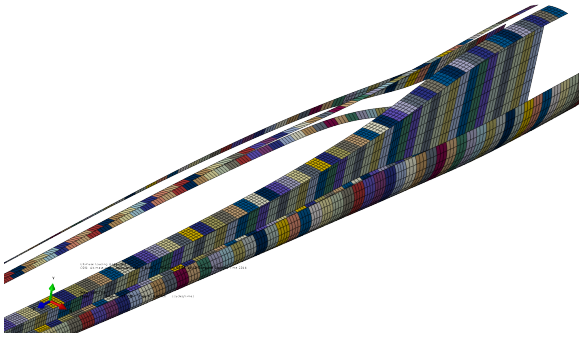

Figure 1. DTU 10 MW wind turbine blade reference model layup partitioning.

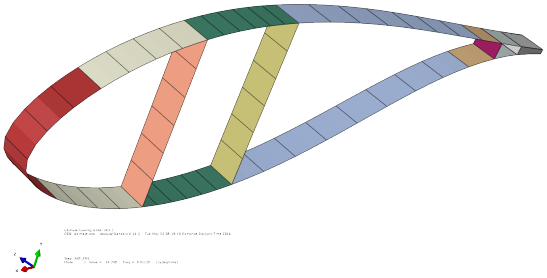

Figure 2. DTU 10 MW wind turbine blade reference model composite layup definition along circumferential partitions.

This study aims to determine the loss of strength in ply-drop areas in a wind turbine blade structure, where material transition discontinuities, abrupt change in bending stiffness, and singular inter-laminar stresses turn them into critical failure prone regions.

2. Methodology

Load combinations outcome have been provided in 27 cross sections along the reference blade, in accordance with IEC 61400-1 Ed.3 [8]. The ultimate load case(1.3)[1] for maximum moment resultant is the prominent design load case. Corresponding forces and moments are distributed over nodal points in cross sections, through defining coupled constraints with respect to nodal distance from the elastic center (figure 3). The resulted displacement field is then applied to a sub-model to investigate the local stress concentrations and damage onset in selected thickness tapered regions as sub-models in ABAQUS (figure 4). Sub-modeling provides finer mesh resolution and use of different set and geometry of elements, while all essential and natural boundary conditions from the main model are inherited over the desired area [13]. Conventional layered shell elements are replaced with solid elements to model the geometrical variations and obtain a local strain distribution in ply-drop areas, especially near the boundaries of the resin

[1] Extreme turbulence model wind conditions with safety factor of 1.35, according to IEC 61400-1 Ed.3.

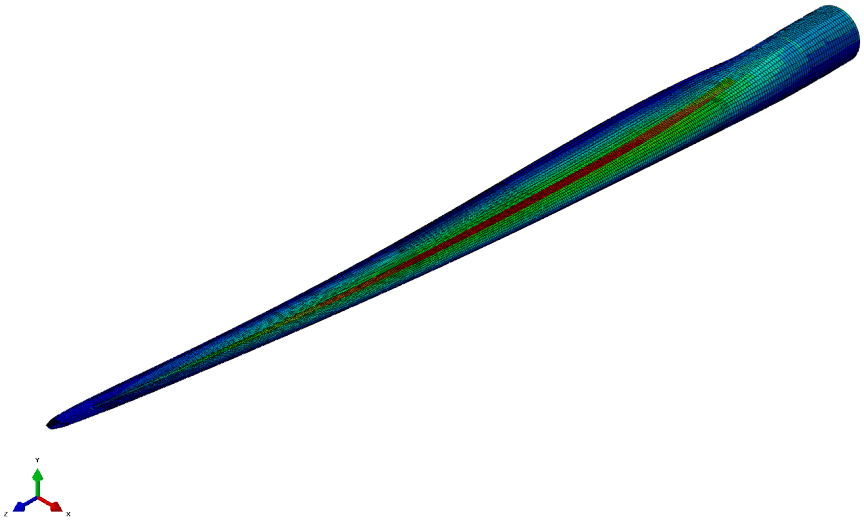

Figure 3. DTU 10 MW offshore wind turbine blade reference model under ultimate design load case(1.3), according to the Guideline approach [12] with an inherent partial safety factor of 1.35 for flap-wise blade bending moment.

rich pocket area. Biaxial and triaxial laminae have been considered as an assembly of individual uni-directional laminae with their corresponding directions, bonded together in interfaces. Large displacements due to blade movements, have been carefully decoupled from internal displacement field. Linear elastic material properties for the constituent materials are mentioned in tables 1-4. Tensile, compressive, and shear strengths of the material that have not been reported in the reference blade document [8] have been derived from the literature by matching the materials elastic moduli [14] (tables 1 and 2).

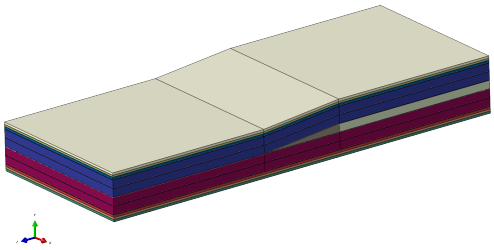

Figure 4. Finite element sub-model of ply-drop effect, to study localized stresses, leading to failure initiation.

Ply stacking of the sub-model which is a 1:10 tapered section of [[-45/0/+45]/0_5/[+45/0/-45]] to [[-45/0/+45]/0_2]$_s$ (figure 4), has to be considered under fatigue loading. Tension and compression fatigue test results from equivalent sample of QQ1[2][3] of the same material with very close mechanical properties is adopted in calculation of residual strength by means of tensile and compressive stress to fatigue life curves in both fiber and transverse directions (figures 5 and 6).

[2] Test specimen series of epoxy and glass fiber with 53% fiber volume with a similar layup to the numerical model of the current study [3].

Table 1. Mechanical properties of the epoxy matrix [8, 14].

Property	Value	Unit
Young's modulus E_m	4.0	GPa
Poisson's ratio ν_m	0.35	...
Shear modulus G_m	1.48	GPa
Mass density ρ_m	1140	kg/m^3
Tensile strength Y_{mt}	0.075	GPa
Compressive strength Y_{mc}	0.150	GPa
Shear strength S_m	0.070	GPa

Table 2. Mechanical properties of E-glass fibers [8, 14].

Property	Value	Unit
Longitudinal Young's modulus E_{f1}	75.0	GPa
Transverse Young's modulus E_{f2}	75.0	GPa
Major Poisson's ratio ν_{12}	0.2	...
In-plane shear modulus G_{f12}	31.25	GPa
Transverse shear modulus G_{f23}	31.25	GPa
Mass density ρ_f	2550	kg/m^3
Longitudinal tensile strength X_{ft}	2.150	GPa
Longitudinal Compressive strength X_{fc}	1.450	GPa

Table 3. Apparent mechanical properties of two uni-directional laminae [8].

Property	Lamina 1	Lamina 2	Unit
Fiber volume fraction V_f	0.50	0.55	...
Young's modulus in fiber direction E_1	39.50	43.05	GPa
Young's modulus in dir. transverse to dir.1 E_2	12.10	13.43	GPa
In-planar shear modulus G_{12}	4.54	5.05	GPa
Out-of-plane shear modulus G_{23}	4.54	5.05	GPa
In-plane Poisson's ratio ν_{12}	0.275	0.268	...
Out-of-plane Poisson's ratio ν_{23}	0.333	0.330	...
Mass density ρ	1845	1915	kg/m^3

A set of modified Hashin-type damage criterion [15], capable of predicting different modes of fatigue failure is employed to model the progressive fatigue damage in the sub model. In order to excess the necessity of performing intensive test numbers, the material properties are considered as function of number of cycles, stress states and stress ratios [6]. A residual strength approach, which considers the material stiffness and strength as a function of time, predicts the remaining fatigue life of a unidirectional ply under a multiaxial state of fatigue stress [6]. Different modes

Table 4. Fiber orientation and apparent mechanical properties of the multi-directional plies [8].

Multi-directional ply	Uniax	Biax	Triax	Unit
Fiber volume fraction V_f	0.55	0.5	0.5	...
Unidirectional lamina	Lamina2	Lamina1	Lamina1	...
0°fibers	95	0	30	%
90°fibers	5	0	0	%
+45°fibers	0	50	35	%
−45°fibers	0	50	35	%
Young's modulus E_1	41.63	13.92	21.79	GPa
Young's modulus E_2	14.93	13.92	14.67	GPa
Shear modulus G_{12}	5.047	11.50	9.413	GPa
Poisson's ratio ν_{12}	0.241	0.533	0.478	...
In-plane shear modulus G_{f12}	31.25	GPa		
Transverse shear modulus $G_{13} = G_{23}$	5.05	4.54	4.54	GPa
Mass density ρ	1915	1845	1845	kg/m^3
Longitudinal tensile failure strain ϵ_1^T	2.10	1.60	2.20	%
Longitudinal Compressive failure strain ϵ_1^C	1.50	1.50	1.80	%

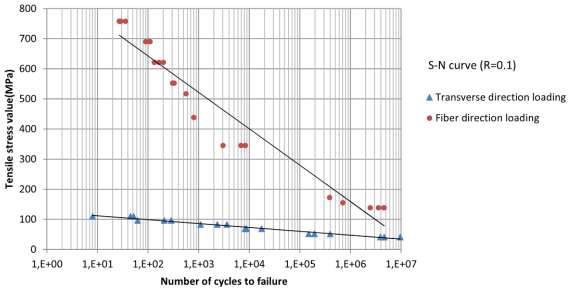

Figure 5. S-N curve for the laminate under different tensile fatigue states(R=0.1) for fiber and transverse directions [3].

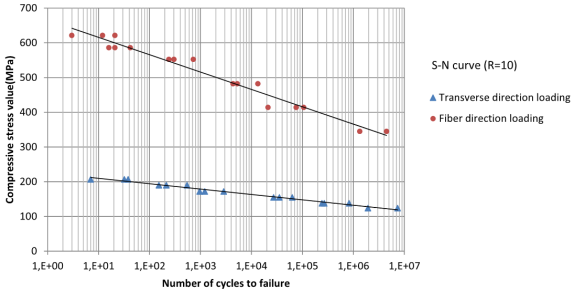

Figure 6. S-N curve for the laminate under different compressive fatigue states(R=10) for fiber and transverse directions [3].

of fatigue failure initiation, propagation, and ultimate damage of a unidirectional ply under uniaxial fatigue loading are calculated by the following criteria [6].

For fiber tension fatigue failure mode ($\sigma_{xx} > 0$), the criterion is:

$$[\frac{\sigma_{xx}}{X_t(n,\sigma,\kappa)}]^2 + [\frac{\frac{\sigma_{xy}^2}{2E_{xy}(n,\sigma,\kappa)} + \frac{3}{4}\delta\sigma_{xy}^4}{\frac{S_{xy}^2(n,\sigma,\kappa)}{2E_{xy}(n,\sigma,\kappa)} + \frac{3}{4}\delta S_{xy}^4(n,\sigma,\kappa)}] + [\frac{\frac{\sigma_{xz}^2}{2E_{xz}(n,\sigma,\kappa)} + \frac{3}{4}\delta\sigma_{xz}^4}{\frac{S_{xz}^2(n,\sigma,\kappa)}{2E_{xz}(n,\sigma,\kappa)} + \frac{3}{4}\delta S_{xz}^4(n,\sigma,\kappa)}] = g_{F+}^2 \quad (1)$$

where $X_t(n,\sigma,\kappa)$, $S_{xy}(n,\sigma,\kappa)$, and $S_{xz}(n,\sigma,\kappa)$ are the fiber residual tensile, in-plane shear, and out of plane shear fatigue strengths, $E_{xy}(n,\sigma,\kappa)$ and $E_{xz}(n,\sigma,\kappa)$ are in-plane and out of plane shear residual fatigue stiffness of a unidirectional ply under uniaxial fatigue loading, and n,σ, κ, and δ account for number of cycles, stress state, stress ratio, and parameter of material nonlinearity, respectively.

For fiber compression fatigue failure mode ($\sigma_{xx} < 0$), the criterion is:

$$[\frac{\sigma_{xx}}{X_c(n,\sigma,\kappa)}] = g_{F-}^2 \tag{2}$$

where $X_c(n,\sigma,\kappa)$ is the fiber compressive residual fatigue strength of a unidirectional ply under uniaxial fatigue loading.

For fiber-matrix shearing fatigue failure mode ($\sigma_{xx} < 0$), the criterion is:

$$[\frac{\sigma_{xx}}{X_c(n,\sigma,\kappa)}]^2 + [\frac{\frac{\sigma_{xy}^2}{2E_{xy}(n,\sigma,\kappa)} + \frac{3}{4}\delta\sigma_{xy}^4}{\frac{S_{xy}^2(n,\sigma,\kappa)}{2E_{xy}(n,\sigma,\kappa)} + \frac{3}{4}\delta S_{xy}^4(n,\sigma,\kappa)}] + [\frac{\frac{\sigma_{xz}^2}{2E_{xz}(n,\sigma,\kappa)} + \frac{3}{4}\delta\sigma_{xz}^4}{\frac{S_{xz}^2(n,\sigma,\kappa)}{2E_{xz}(n,\sigma,\kappa)} + \frac{3}{4}\delta S_{xz}^4(n,\sigma,\kappa)}] = g_{FM}^2 \tag{3}$$

For matrix tension fatigue failure mode ($\sigma_{yy} > 0$), the criterion is:

$$[\frac{\sigma_{yy}}{Y_t(n,\sigma,\kappa)}]^2 + [\frac{\frac{\sigma_{xy}^2}{2E_{xy}(n,\sigma,\kappa)} + \frac{3}{4}\delta\sigma_{xy}^4}{\frac{S_{xy}^2(n,\sigma,\kappa)}{2E_{xy}(n,\sigma,\kappa)} + \frac{3}{4}\delta S_{xy}^4(n,\sigma,\kappa)}] + [\frac{\sigma_{yz}}{S_{yz}(n,\sigma,\kappa)}]^2 = g_{M+}^2 \tag{4}$$

where $Y_t(n,\sigma,\kappa)$ and $S_{yz}(n,\sigma,\kappa)$ are residual transverse tensile and out of plane shear fatigue strengths of a unidirectional ply under uniaxial fatigue loading, respectively.

and finally for matrix compression fatigue mode ($\sigma_{yy} < 0$), we can write:

$$[\frac{\sigma_{yy}}{Y_c(n,\sigma,\kappa)}]^2 + [\frac{\frac{\sigma_{xy}^2}{2E_{xy}(n,\sigma,\kappa)} + \frac{3}{4}\delta\sigma_{xy}^4}{\frac{S_{xy}^2(n,\sigma,\kappa)}{2E_{xy}(n,\sigma,\kappa)} + \frac{3}{4}\delta S_{xy}^4(n,\sigma,\kappa)}] + [\frac{\sigma_{yz}}{S_{yz}(n,\sigma,\kappa)}]^2 = g_{M-}^2 \tag{5}$$

where $Y_c(n,\sigma,\kappa)$ is the transverse compressive residual fatigue strength of a unidirectional ply under uniaxial fatigue loading. In each of the equations 1 to 5, failure occurs when g_* value on the right hand side of the criterion exceeds 1. This means that the material properties under the increasing number of cycles decrease to a level that fail to withstand the applied stresses.

The residual strength in the material by the number of fatigue loadings cycles with random stress ratio is formulated as [6]:

$$R(n,\sigma,\kappa) = [1 - (\frac{\log(n) - \log(0.25)}{\log(N_f - \log(0.25)})^{\beta}]^{\frac{1}{\alpha}}(R_s - \sigma) + \sigma \tag{6}$$

where R_s is static strength, N_f is the fatigue life at σ, and α and β are experimental curve fitting parameters.

A similar equation for the stiffness degradation by number of cycles is rearranged as [16]:

$$E(n,\sigma,\kappa) = [1 - (\frac{\log(n) - \log(0.25)}{\log(N_f - \log(0.25)})^{\lambda}]^{\frac{1}{\gamma}}(E_s - \sigma/\varepsilon_f) + \sigma/\varepsilon_f \tag{7}$$

where E_s is static stiffness, ε_f is average strain to failure, and λ and γ are experimental curve fitting parameters.

3. Results and Discussion

Ply-drop configurations have been modelled on two extreme stress concentration positions throughout the cap sections on pressure and suction sides of the reference wind turbine blade. The sub-model with continuum solid elements of quadratic order inherits the displacement field from the global model and shows the local distribution of different stress states around the dropped thickness area (figures 7 and 8). Average nodal stress components of elements with high stress concentrations in the vicinity of resin pocket (table 5) are input in equations 1-5 to calculate the failure index for each fatigue failure mode. Final failure mechanism and remaining life is estimated by replacing the virgin static strengths in the criteria by residual static strength of the material [17].

Table 5. Average stress values at points of stress for calculating the fiber/matrix fatigue failure index.

Stress component	suction side	pressure side	Unit
σ_{xx}	-83	224	MPa
σ_{xy}	-27	7	MPa
σ_{xz}	-12.6	-24.4	MPa
σ_{yy}	-31.3	-45	MPa
σ_{yz}	-2	-45	MPa
σ_{zz}	29.8	41.06	MPa

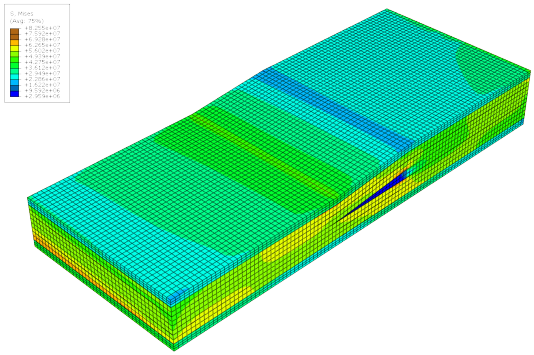

Figure 7. Axial stress distribution in ply-drop sub-model under ultimate tensile loading within pressure side of the cap section.

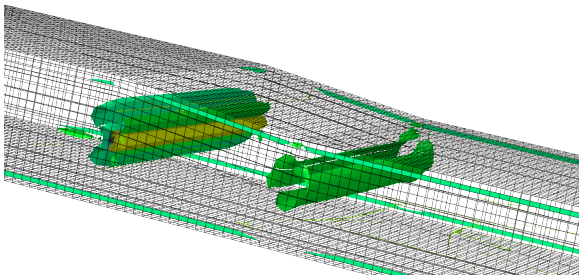

Figure 8. Interlaminar stress concentrations about resin pocket edges in ply-drop area within suction side of the cap section.

Residual strength and stiffness throughout the life-time of blade have been approximated by curve-fitting over existing Wöhler curve data and equations 6-7. Residual strength has been calculated in 20%, 60%, and 80% of the normalized fatigue life and introduced into the fatigue failure criterions (figure 9). Degradation of the material characteristics over the time, resembles fatigue loading effects and influences each failure criterion in a particular way. Failure index foremost hits the limits for delamination and fiber tension fatigue in pressure side of the blade, while matrix compression and delamination fatigue failure modes are prominent modes in suction side. Fiber tension fatigue failure mode is observed to be more sensitive to the cyclic loading with a more steep trend during the time. Other failure modes are almost constant during 80% of the life-time and increase abruptly throughout the last 20%. The method calculates an

approximation of the remaining life-cycles for the laminate after undergoing definite load level at any stage of the composite, from damage initiation until its evolution and final failure.

4. Conclusions

Fatigue failure in ply-drop areas of wind turbine blades has been modelled and studied through a progressive and multi-axial fatigue damage modeling in developed Hashin criteria. Damage state has been predicted at different load levels and number of cycles. The damage nucleation by delamination near the resin rich pocket area complies with analytical solutions [18] and available experimental results. The potential of the study in reducing the required number of experimental data for different loading scenarios, improves the design process of new wind turbine blade configurations.

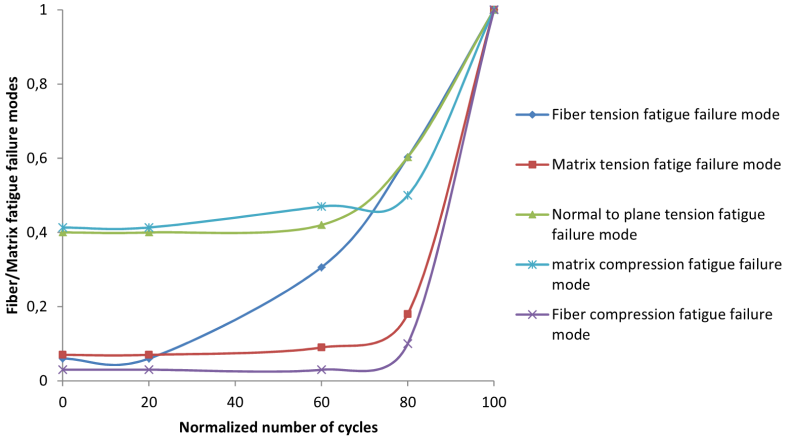

Figure 9. fatigue index with respect to the normalized number of cycles for the fatigue modes of fiber and matrix.

References

[1] Llanos A and Vizzini A 1992 *Journal of Composite Materials* **26** 1968–1983
[2] He K, Hoa S V and Ganesan R 2000 *Composites Science and Technology* **60** 2643–2657
[3] Mandell J and Samborsky D 2010 *Sandia National Laboratories* 1–198
[4] Degrieck J and Van Paepegem W 2001 *Applied Mechanics Reviews* **54** 279–300
[5] Liu Y and Mahadevan S 2013 *Fatigue of Composite Materials* **3** 3
[6] Shokrieh M M and Lessard L B 2000 *Journal of Composite Materials* **34** 1056–1080
[7] MINNETYAN L and CHAMIS C 2013 *Fatigue of Composite Materials* **3** 3
[8] Bak C, Zahle F, Bitsche R, Kim T, Yde A, Henriksen L, Andersen P B, Natarajan A and Hansen M H 2014 *Wind Energy*
[9] Version A 2014 *Analysis Users Guide, Dassault Systems*
[10] Chamis C C 1984 *SAMPE Quarterly* **15** 14–23
[11] Jones R M 1998 *Mechanics of composite materials* (CRC press)
[12] Guideline G W 2010 *Hamburg: Germanischer Lloyd Wind Energie Gmb H*
[13] Dassault Systèmes Simulia 2014 1146
[14] Soden P, Hinton M and Kaddour A 1998 *Composites Science and Technology* **58** 1011–1022
[15] Hashin Z 1980 *Journal of applied mechanics* **47** 329–334
[16] Naderi M and Maligno A 2013 *Journal of Composite Materials* **47** 475–484
[17] Hashin Z 1981 *International Journal of Fracture* **17** 101–109
[18] Pagano N J 2012 *Interlaminar response of composite materials* (Elsevier)